BJP British Journal of Pharmacology

DOI:10.1111/bph.12003
www.brjpharmacol.org

RESEARCH PAPER

Agonists with supraphysiological efficacy at the muscarinic M_2 ACh receptor

R Schrage[1], WK Seemann[1], J Klöckner[2], C Dallanoce[3], K Racké[4], E Kostenis[5], M De Amici[3], U Holzgrabe[2] and K Mohr[1]

[1]*Pharmacology & Toxicology Section, Institute of Pharmacy, University of Bonn, Bonn, Germany,* [2]*Department of Pharmaceutical Chemistry, Institute of Pharmacy, University of Würzburg, Würzburg, Germany,* [3]*Dipartimento di Scienze Farmaceutiche, Sezione di Chimica Farmaceutica 'Pietro Pratesi', Università degli Studi di Milano, Milano, Italy,* [4]*Institute of Pharmacology & Toxicology, University of Bonn, Bonn, Germany, and* [5]*Molecular-, Cellular-, and Pharmacobiology Section, Institute of Pharmaceutical Biology, University of Bonn, Bonn, Germany*

Correspondence
Klaus Mohr, Pharmacology & Toxicology Section, Institute of Pharmacy, University of Bonn, Gerhard-Domagk-Straße 3, 53121 Bonn, Germany. E-mail: k.mohr@uni-bonn.de

Keywords
Superagonism; GPCRs; muscarinic ACh receptors; iperoxo; efficacy; cell signalling; biased agonism; label-free technologies; dynamic mass redistribution

Received
26 March 2012
Revised
18 September 2012
Accepted
19 September 2012

BACKGROUND AND PURPOSE
Artificial agonists may have higher efficacy for receptor activation than the physiological agonist. Until now, such 'superagonism' has rarely been reported for GPCRs. Iperoxo is an extremely potent muscarinic receptor agonist. We hypothesized that iperoxo is a 'superagonist'.

EXPERIMENTAL APPROACH
Signalling of iperoxo and newly synthesized structural analogues was compared with that of ACh at label-free M_2 muscarinic receptors applying whole cell dynamic mass redistribution, measurement of G-protein activation, evaluation of cell surface agonist binding and computation of operational efficacies.

KEY RESULTS
In CHO-hM_2 cells, iperoxo significantly exceeds ACh in G_i/G_s signalling competence. In the orthosteric loss-of-function mutant M_2-Y104$^{3.33}$A, the maximum effect of iperoxo is hardly compromised in contrast to ACh. 'Superagonism' is preserved in the physiological cellular context of MRC-5 human lung fibroblasts. Structure–signalling relationships including iperoxo derivatives with either modified positively charged head group or altered tail suggest that 'superagonism' of iperoxo is mechanistically based on parallel activation of the receptor protein via two orthosteric interaction points.

CONCLUSION AND IMPLICATIONS
Supraphysiological agonist efficacy at muscarinic M_2 ACh receptors is demonstrated for the first time. In addition, a possible underlying molecular mechanism of GPCR 'superagonism' is provided. We suggest that iperoxo-like orthosteric GPCR activation is a new avenue towards a novel class of receptor activators.

LINKED ARTICLE
This article is commented on by Langmead and Christopoulos, pp. 353–356 of this issue. To view this commentary visit http://dx.doi.org/10.1111/bph.12142

Abbreviations
[^{35}S]GTPγS, guanosine 5′-(γ-thio)triphosphate; [^{3}H]NMS, [^{3}H]N-methylscopolamine; CHO-hM_2 (CHO-hM_2-Y104$^{3.33}$A) cells, Chinese hamster ovary cells stably expressing the human gene for muscarinic M_2 wild type (M_2-Y104$^{3.33}$A mutant) receptor; DMR, dynamic mass redistribution; IP-C1, iperoxo; Oxo M, oxotremorine M; PTX, pertussis toxin

Introduction

The superfamily of GPCRs has a key role in biology and drug therapy. Being integrated into the cytoplasmic membrane, GPCRs serve for sensing the cellular environment and for appropriate adjustment of cell function. Pharmacological modulation of GPCR function is a mainstay of drug therapy (Lagerström and Schiöth, 2008). GPCR architecture is charac-

terized by seven transmembrane helices linked by extracellular and intracellular loops (7TMR, 7 helical transmembrane receptors). GPCR activation by an extracellular stimulus is relayed into intracellular loop rearrangement and subsequent selective activation of cellular adaptor proteins. These regulate intracellular signalling pathways, thus orchestrating a cellular response (DeWire *et al.*, 2007).

On the molecular level, GPCRs behave as dynamically fluctuating macromolecules that adopt ensembles of tertiary conformations (Deupi and Kobilka, 2010; Kenakin and Miller, 2010). Binding of the endogenous messenger molecule tunes the frequency distribution of conformations from an inactive into an active pattern. The activator-bound receptor may oscillate between conformations that differ in selectivity and efficacy for adaptor protein activation. The question arises whether evolution has optimized messenger molecule/receptor interactions to achieve the maximum signalling output, or, on the contrary, whether artificial molecules can be designed that surpass the endogenous activator in efficacy for receptor activation. Such 'superagonists' would open new perspectives in drug design and provide novel insight into physiological receptor function. For instance, agonists that stabilize a receptor conformation of maximum efficacy should be valuable tools in receptor crystallography.

Iperoxo is a muscarinic ACh receptor agonist with outstanding potency (Dallanoce *et al.*, 1999). The compound has recently gained increasing interest as an essential building block for a novel class of GPCR modulators (Antony *et al.*, 2009; Mohr *et al.*, 2010; Valant *et al.*, 2012). These orthosteric/allosteric (dualsteric) hybrid agonists combine receptor subtype preference and signalling pathway selectivity. Iperoxo binds to the orthosteric ACh site of the receptor protein. In striking contrast to conventional muscarinic agonists, linkage of voluminous allosteric residues to the iperoxo molecular skeleton does not severely compromise agonistic efficacy (compare Disingrini *et al.*, 2006 with Antony *et al.*, 2009). Therefore, iperoxo has been addressed phenomenologically as a 'high fidelity agonist' (Mohr *et al.*, 2010).

To find out whether iperoxo has a higher efficacy than the physiological agonist ACh, we designed and synthesized some systematically modified derivatives of iperoxo and characterized their signalling in comparison with the parent compound and conventional agonists at the M_2 muscarinic receptor subtype applying a variety of assays. Findings indicate that iperoxo and some of its analogues are significantly superior to the physiological transmitter ACh with respect to converting receptor occupancy into a cellular response. We demonstrate that targeted disruption of ligand–receptor interactions by alkylation at either end of the iperoxo molecule abolishes elevated efficacy of iperoxo and results in ACh-like signalling properties. However, whereas the polar head group of iperoxo requires addition of a *pentyl* chain to obstruct elevated efficacy, introduction of one *methyl* group into the opposite heterocyclic portion of the molecule is sufficient to erase enhanced efficacy.

Thus, our findings suggest that iperoxo's higher efficacy compared with ACh is based on an ancillary interaction of the iperoxo molecule with the orthosteric binding pocket, additional to the classical interaction of the ammonium head group of muscarinic agonists with the receptor. Thus, our study gives insight into a molecular mechanism underlying more-than-physiological efficacy at a GPCR.

Methods

Test compounds and media

ACh iodide, oxotremorine M iodide, atropine sulfate and *N*-methylscopolamine bromide were obtained from Sigma-Aldrich Chemie (Steinheim, Germany). [^{35}S]GTPγS and [^{3}H]*N*-methylscopolamine bromide ([^{3}H]NMS) were from PerkinElmer Life and Analytical Sciences (Homburg, Germany).

Cell culture media were purchased from Sigma-Aldrich (Taufkirchen, Germany) and Invitrogen (Darmstadt, Germany). All experiments conducted with living cells were carried out in HBSS buffer (Invitrogen, Darmstadt, Germany) supplemented with 20 mM HEPES (pH 7.0).

Drug and molecular target nomenclature conforms to the BJP's *Guide to Receptors and Channels* (Alexander *et al.*, 2011).

Chemical synthesis

Iperoxo (IP-C1) and its building block, IP-H (Figure 1), were synthesized as described elsewhere (Klöckner *et al.*, 2010). A detailed description of the synthesis of the novel congeners IP-C3, IP-C5, and C1-IP-C1 (Figure 1) is given in the Supplementary Information (see 'Chemistry' and Supplementary Figure S1).

Cell culture

We used Flp-In™-CHO cells stably expressing either the hM_2 receptor (CHO-hM_2 cells) or the hM_2-Y104$^{3.33}$A (Ballesteros and Weinstein nomenclature in superscript) mutant receptor (CHO-hM_2-Y104$^{3.33}$A cells) and a human lung fibroblast cell line (MRC-5). CHO cells were cultured in Ham's nutrient mixture F-12 (Ham's F-12) supplemented with 10% (v/v) fetal calf serum (FCS), 100 U mL^{-1} penicillin, 100 μg mL^{-1} streptomycin and 2 mM L-glutamine. MRC-5 human lung fibroblasts were grown in Eagle's minimal essential medium (MEM) with Earle's Salts and L-glutamine (PAA Laboratories GmbH, Cölbe, Germany) supplemented with 10% FCS, 0.1 mM non-essential amino acids (PAA Laboratories GmbH), 1.0 mM sodium pyruvate (PAA Laboratories GmbH), 100 U mL^{-1} penicillin and 100 μg mL^{-1} streptomycin. All cells were grown in a humidified incubator at 37°C and 5% CO_2, and passaged by trypsinization at nearly confluence.

Membrane preparation

For membrane preparations, stably transfected CHO cells were grown to 90% confluence and treated with fresh medium containing 5 mM sodium butyrate for 18–24 h. On the day of membrane preparation, medium was aspirated, and CHO cells were detached mechanically in 2.4 mL ice-cold harvesting buffer (20 mM HEPES, 10 mM Na_2EDTA, pH 7.4) with a cell scraper (Sarstedt AG & CO, Nümbrecht, Germany). The cell suspension was homogenized using a Polytron homogenizer (2 × 25 s, level 6). The suspension of destroyed cells was centrifuged (10 min, 40 000 × *g*, 2°C), and the pellet was resuspended in storage buffer (20 mM HEPES, 0.1 mM Na_2EDTA, pH 7.4). This centrifugation step was repeated

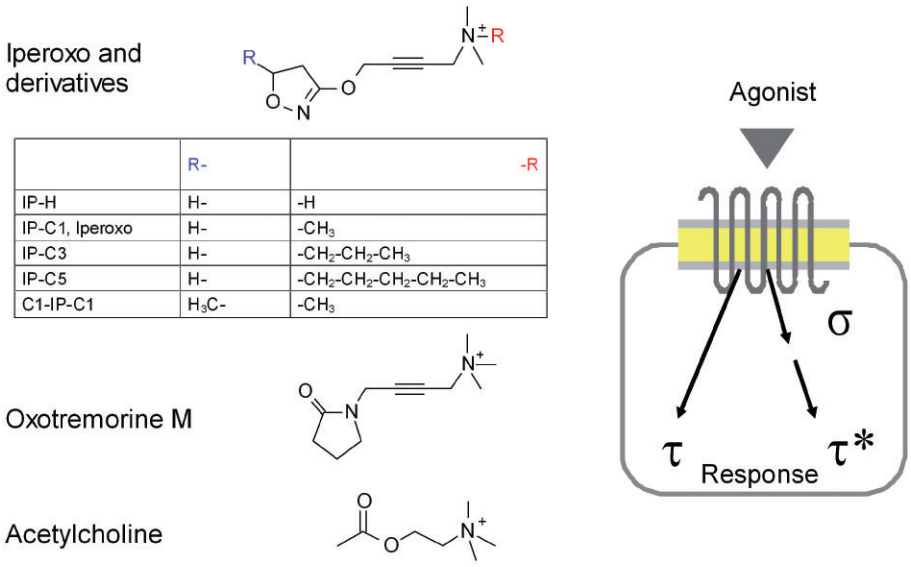

Figure 1

Orthosteric muscarinic agonists and parameters for quantifying their signalling efficacy. Left panel: Structures of iperoxo, its derivatives and conventional orthosteric muscarinic agonists including the physiological activator ACh. Right panel: τ (tau) reflects the operational efficacy between the agonist-bound receptor and a cellular response. τ can be subdivided into the components σ (sigma) and τ^*, with σ denoting the ability of an agonist to induce a signalling competent receptor conformation relative to ACh and τ^* indicating the cellular capacity for downstream signalling (Rajagopal *et al.*, 2011).

twice. The remaining pellet was resuspended in an adequate amount of [^{35}S]GTPγS assay buffer (12.5 mM HEPES, 12.5 mM $MgCl_2$, 125 mM NaCl, pH 7.4) and stored at –80°C.

Whole cell binding

Whole cell binding experiments were conducted to quantify receptor surface expression according to DeBlasi *et al.* (1989) and to measure agonist binding affinities.

Therefore, CHO cells were seeded on cell culture dishes and grown for 2 days. On the day of experiment, cells were harvested and resuspended in HBSS buffer containing 20 mM HEPES (pH 7.0); 150 000 cells mL^{-1} were incubated with 0.2 nM [^{3}H]NMS and different concentrations of either unlabelled NMS or agonist in a 96-well microtiterplate (Thermo Scientific ABgene, Germany) in a final volume of 500 µL at 28°C, for 2 h to reach equilibrium (half-life of [^{3}H]NMS dissociation: 2.1 ± 0.1 min; mean value ± SEM; n = 3). Experiments were terminated by rapid vacuum filtration using a Tomtec Harvester, and filter-bound radioactivity was calculated by solid scintillation. Non-specific binding was determined in the presence of 10 µM atropine and did never exceed 2%. For chemical knock-out of G_i-proteins, cells were pretreated with 100 ng mL^{-1} pertussis toxin (PTX) (Biotrend GmbH, Cologne, Germany) for 16–24 h.

Human lung fibroblasts (MRC-5) were grown to confluence in cell culture flasks. On the day of experiment, cells were harvested and resuspended in HBSS buffer supplemented with 20 mM HEPES (pH 7.0). 100 000 cells mL^{-1} were incubated with 0.2 nM [^{3}H]NMS and either unlabelled NMS or agonists at different concentrations in a final volume of 1.5 mL in reaction tubes at 28°C for 2 h to reach equilibrium. Filtration was performed with a Brandel Harvester (Brandel, Gaithersburg, MD) as described elsewhere (Tränkle *et al.*, 1996), and non-specific binding was determined in the presence of 10 µM atropine and did never exceed 6%.

[^{35}S]GTPγS binding assay

[^{35}S]GTPγS binding experiments were conducted as described previously (Jäger *et al.*, 2007). Briefly, homogenates of membranes from CHO-hM_2 wild-type or CHO-hM_2-Y104$^{3.33}$A cells (40 µg mL^{-1}) were incubated with 0.07 nM [^{35}S]GTPγS and maximum agonist-induced [^{35}S]GTPγS incorporation was measured after 1 h.

Dynamic mass redistribution (DMR)

A detailed protocol to measure DMR in CHO and MRC-5 cells is published in Schröder *et al.* (2011) and Lamyel *et al.* (2011) respectively. Briefly, cells were grown to confluence for 20–24 h on Epic® biosensor 384-well microplates. On the day of experiment, cells were washed twice with HBSS containing 20 mM HEPES (pH 7.0) and kept for 2 h in the Epic® reader at 28°C. DMR was monitored before (baseline read) and after the addition of compound solutions for 3600 s. For experiments to quantify G_s–protein activation, cells were pretreated with PTX (100 ng mL^{-1}) for 18–24 h.

Data analysis

Agonist-induced DMR was measured by the quantification of the maximal peak between 0 and 1800 s after compound addition as described earlier (Schröder *et al.*, 2010). As demonstrated by Schröder *et al.* (2011), the shape of the concentration–effect curve is 'stable' irrespective of whether the DMR-response is recorded (i) at differing time points

(1200s, 2400s, 3600 s), (ii) as the peak of the signal (as used in this paper), (iii) as the slope of the signal or (iv) as the area under the signal between 0 s and 3600 s (Schröder *et al.*, 2011).

Nonlinear regression analyses were performed using Prism 4.02 (GraphPad Software, San Diego, CA). Equilibrium binding data were analysed by a four-parameter logistic function yielding IC_{50} values, which were subsequently transformed into apparent equilibrium dissociation constants K_A using the Cheng–Prusoff correction as described previously (Antony *et al.*, 2009). Data obtained from [^{35}S]GTPγS binding and DMR assays were fitted by a four parameter logistic function to estimate the potency (pEC_{50}) and maximum inducible effect (E_{max}) by the particular agonists. Additionally, mean values from functional experiments with CHO-hM_2 wild-type and MRC-5 cells were analysed by the operational model of agonism (Black and Leff, 1983; and for instance Suratman *et al.*, 2011), to estimate operational efficacies τ with the following equation:

$$E = \frac{E_{max}\tau^n[A]^n}{\tau^n[A]^n + ([A]+K_A)^n}$$

E: response

E_{max}: maximal response of the system

τ: operational efficacy; indicating how efficient agonist binding is transduced into a response

(n) slope parameter

[A]: concentration of agonist

K_A: agonist's dissociation constant fixed at values derived from radioligand binding assays (see above)

To estimate operational efficacies of downward deflected curves, data points were mirrored horizontally.

Operational efficacies were transformed into the effective signalling (σ) for expressing signalling of test compounds relative to that of the physiological activator ACh (Rajagopal *et al.*, 2011):

$$\sigma = \log\left(\frac{\tau_{lig}}{\tau_{ACh}}\right)$$

Statistics

Data are shown as means ± SEM for n observations. Comparisons of two single means and groups of means were performed using an unpaired Student's t-test and a one-way ANOVA with Bonferroni's multiple comparison tests respectively. Whenever curves were fitted with the four-parameter logistic equation and the slope of the curve differed significantly from 1 or −1 (F-test, $P < 0.05$), this is indicated in the respective table.

Results

Targeted modifications of iperoxo serve to understand structure–function relationships

Comparison of the structures of iperoxo ('IP-C1') and oxotremorine M suggests that iperoxo's outstanding potency resides in its Δ^2-isoxazolinyl-ether substituent, as both compounds share the trimethylammonium head group and the linker chain (Figure 1). The quaternary head group is essential for the receptor interaction of ACh and related conventional agonists (Lu *et al.*, 2002). When one of the methyl residues of the head group in iperoxo is replaced by a hydrogen (yielding 'IP-H', Figure 1), potency declines in isolated tissue preparations by about 1–2 log units (Dallanoce *et al.*, 1999). In order to further clarify the role of the head group for the signalling of iperoxo, we enlarged the head group by replacing a methyl substituent by either *n*-propyl or *n*-pentyl, yielding 'IP-C3' and 'IP-C5' respectively (Figure 1). In addition, the Δ^2-isoxazolinyl-ether substituent was altered by methylation in position 5, yielding 'C1-IP-C1' to gain deeper insight into the function of iperoxo's characteristic tail group.

Test compound signalling was evaluated by the operational efficacy 'tau, τ' (Black and Leff, 1983) of an agonist for inducing a cellular response (Figure 1). This parameter can be subdivided into the ability of an agonist to induce a signalling-competent receptor conformation (σ) and the capacity of the cell for downstream propagation of the signal (τ^*, Rajagopal *et al.*, 2011).

Iperoxo has unique potency for triggering muscarinic receptor signalling

The muscarinic ACh receptor of the M_2 subtype is known to activate G_i- and G_s-proteins (Haga *et al.*, 1985; Michal *et al.*, 2001). We applied cellular DMR to monitor M_2 receptor function in CHO cells stably transfected to express this receptor (CHO-hM_2). DMR is a powerful label-free optical biosensor-based technology for the identification and quantification of G-protein-dependent signalling (Schröder *et al.*, 2010; 2011). We used the maximal (peak) DMR-response between 0 and 1800 s. Iperoxo caused concentration-dependent positive DMR (Figure 2A, 'ctr'), which reflects G_i pathway activation in CHO-hM_2 cells (Schröder *et al.*, 2010). Pretreatment with PTX irreversibly inhibits G_i-proteins and uncovers G_s signalling (Figure 2A, 'PTX'). For all agonists tested, M_2 receptor-mediated G_s activation requires higher agonist concentrations than G_i activation (for original traces obtained with ACh, see Supplementary Figure S2). This explains why DMR concentration–effect curves of M_2 receptor-mediated signalling predominantly reflect G_i activation. Concentration–effect curves (Figure 2B) demonstrate that iperoxo shares same maximum G_i/G_s effects with the other test compounds. However, with respect to potency, iperoxo widely surpasses ACh, oxotremorine M and the iperoxo derivatives irrespective of the signalling pathway (Figure 2B and Table 1).

For sake of comparison and in addition to DMR, we measured [^{35}S]GTPγS-accumulation in CHO-hM_2 cell membranes as a functional G_i readout (Milligan, 2003) that is close to the receptor and directly linked to agonist-induced receptor activation. Again, iperoxo shares the same maximum of effect with the other test compounds but surpasses these in potency to a similar extent as in the DMR experiments (Table 2). Test compound potencies did not differ between [^{35}S]GTPγS binding and DMR experiments except for IP-H and oxotremorine M. Surprisingly, oxotremorine M was almost 10-fold more potent in [^{35}S]GTPγS binding assays, resulting in a high operational efficacy with respect to [^{35}S]GTPγS (Table 2A) but not DMR (Table 1), which cannot be explained at present. Of note, Mistry *et al.*, (2005) observed an enhanced efficacy of oxotremorine M relative to

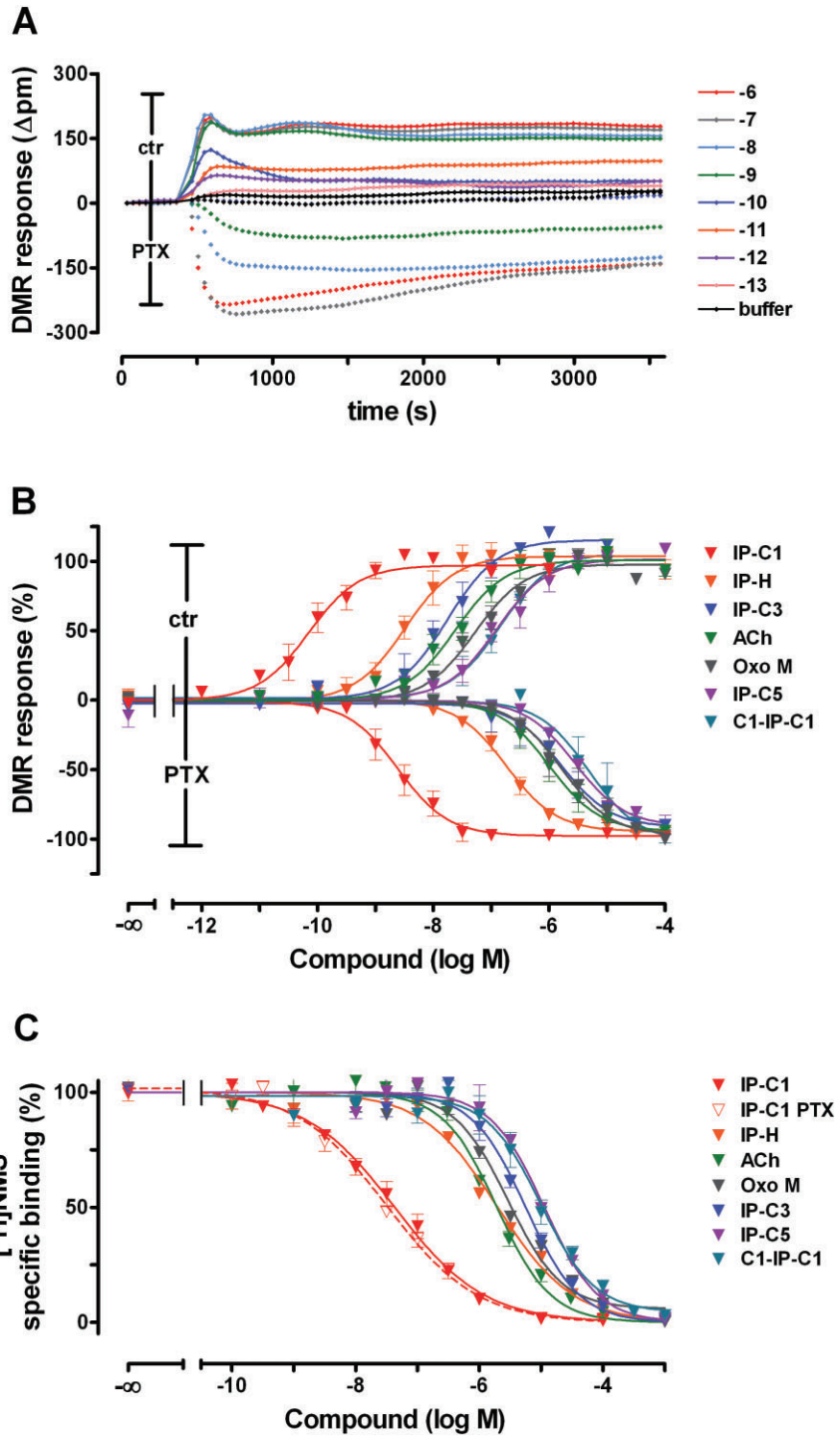

Figure 2

Whole cell response to and cell surface receptor binding of the indicated test compounds in CHO-hM_2. (A) Original recordings of iperoxo-induced DMR (expressed as Δpm wavelength shift) from a representative experiment. CHO-hM_2 cells display positive DMR including a characteristic G_i-peak under normal conditions ('ctr', upper panel) or negative DMR after pretreatment with PTX (lower panel) to inactivate G_i and thereby uncover G_s–protein signalling. Shown are mean values of quadruplicate determinations from one experiment out of six with similar results. SEM was always below 20 pm. (B) Concentration–DMR curves for G_i and G_s signalling (upward and downward deflected curves, respectively) of the indicated test compounds. Curve fitting is based on data from individual experiments (A) that were normalized to the respective maximum response induced by iperoxo. Shown are means ± SEM of three to six independent experiments conducted in quadruplicate. (C) Cell surface binding of the indicated muscarinic agonists as reflected by displacement of the radiolabelled orthosteric antagonist NMS. As representatively shown for iperoxo, PTX pretreatment does not affect agonist binding characteristics. Shown are means ± SEM of three to eight independent experiments conducted in triplicate. Binding data for ACh and IP-C1 were taken from Bock *et al.* (2012).

Table 1

DMR in CHO-hM$_2$ cells induced by muscarinic agonists

Compound	pEC_{50} Control conditions	Hill slope Control conditions	Log τ Control conditions	Compound	pEC_{50} PTX	Hill slope PTX	Log τ PTX
ACh (*n* = 4)	7.60 ± 0.16	0.92 ± 0.20	1.80 ± 0.07	**ACh (*n* = 4)**	6.00 ± 0.20	–0.94 ± 0.18	0.41 ± 0.04
Oxo M (*n* = 5)	7.23 ± 0.13	0.89 ± 0.15	1.58 ± 0.07	**OxoM (*n* = 4)**	5.70 ± 0.27	–1.15 ± 0.14	0.56 ± 0.04
IP-C1 (*n* = 6)	10.10 ± 0.22	0.89 ± 0.15	2.64 ± 0.08	**IP-C1 (*n* = 6)**	8.44 ± 0.20	–0.99 ± 0.15	1.15 ± 0.07
IP-H (*n* = 5)	8.47 ± 0.11	1.49 ± 0.39	2.67 ± 0.08	**IP-H (*n* = 6)**	6.76 ± 0.11	–1.08 ± 0.13	0.88 ± 0.04
IP-C3 (*n* = 4)	7.74 ± 0.25	0.92 ± 0.18	2.53 ± 0.08	**IP-C3 (*n* = 4)**	5.88 ± 0.24	–1.00 ± 0.18	0.53 ± 0.04
IP-C5 (*n* = 6)	6.86 ± 0.19	0.75 ± 0.15	1.86 ± 0.06	**IP-C5 (*n* = 4)**	5.53 ± 0.05	–1.15 ± 0.14	0.56 ± 0.04
C1-IP-C1 (*n* = 3)	6.80 ± 0.19	0.92 ± 0.15	1.80 ± 0.07	**C1-IP-C1 (*n* = 3)**	5.44 ± 0.38	–0.94 ± 0.39	0.45 ± 0.04

Agonist concentrations inducing a half-maximal DMR effect (minus log values, pEC_{50}) and slope factors were obtained by fitting the four parameter logistic equation to data from individual experiments shown in Figure 2B. Operational efficacies (log values, log τ) were derived from DMR-data and whole cell binding constants (cf. Table 3) according to the operational model of agonism. Shown data are means ± SEM from *n* (as indicated below the agonist name) independent experiments conducted in quadruplicate.

Table 2

[^{35}S]GTPγS-accumulation induced by selected muscarinic agonists in membrane homogenates of CHO-hM$_2$ wild type and CHO-hM$_2$-Y104$^{3.33}$A cells

Compound	pEC_{50}	E_{max} (%)	Hill slope	log τ
(A) M$_2$ wild-type receptor				
ACh (*n* = 8)	7.40 ± 0.09	103 ± 3	0.75[a] ± 0.07	1.68 ± 0.06
Oxo M (*n* = 3)	8.07 ± 0.19	103 ± 3	0.67[a] ± 0.09	2.35 ± 0.07
IP-C1 (*n* = 12)	9.80 ± 0.09	99 ± 2	1.05 ± 0.08	2.33 ± 0.07
IP-H (*n* = 3)	7.97 ± 0.21	108 ± 7	1.49 ± 0.60	2.15 ± 0.06
IP-C3 (*n* = 3)	7.63 ± 0.07	102 ± 2	0.77[a] ± 0.06	2.27 ± 0.06
IP-C5 (*n* = 6)	6.64 ± 0.12	88[b] ± 3	0.80 ± 0.14	1.41 ± 0.06
C1-IP-C1 (*n* = 3)	6.80 ± 0.11	99 ± 3	0.86 ± 0.13	1.67 ± 0.08
(B) M$_2$-Y104$^{3.33}$A receptor				
ACh (*n* = 4)	4.15 ± 0.20	43[b,c] ± 2	1.25 ± 0.20	n.a.
Oxo M (*n* = 3)	5.23 ± 0.07	27[b,c] ± 1	1.69 ± 0.47	n.a.
IP-C1 (*n* = 5)	5.56 ± 0.05	100 ± 2	0.57[a] ± 0.03	n.a.
IP-H (*n* = 4)	5.11 ± 0.16	73[b] ± 3	0.84 ± 0.14	n.a.
IP-C3 (*n* = 7)	6.19 ± 0.07	81[b] ± 3	0.88 ± 0.16	n.a.
IP-C5 (*n* = 6)	5.94 ± 0.08	72[b] ± 2	0.89 ± 0.13	n.a.
C1-IP-C1 (*n* = 3)	4.38 ± 0.09	36[b,c] ± 1	0.85 ± 0.14	n.a.

Agonist concentrations for inducing a half maximal effect in [^{35}S]GTPγS binding experiments (minus log values, pEC_{50}), maximum agonist effects (E_{max}) and slope factors were obtained by fitting the four parameter logistic equation to data from individual experiments conducted with (A) membranes from CHO-hM$_2$ wild type and (B) from CHO-hM$_2$-Y104$^{3.33}$A cells. E_{max} values are in % of the maximum response induced by iperoxo in the respective experiment.

Operational efficacies (log values, log τ) were obtained by fitting the same data points to equation 1 with a fixed agonist binding dissociation constant K_A (see Table 3). In case of the mutant, extremely low agonist binding affinities prevented calculation of K_A and efficacies (B). Data are means ± SEM from *n* (as indicated below the agonist name) independent experiments conducted in quadruplicate.

[a]Significantly different from 1 ($P < 0.05$).

[b]Significantly different from the respective maximum response induced by iperoxo at CHO-hM$_2$ wild type (upper panel) or CHO-hM$_2$-Y104$^{3.33}$A (lower panel) receptors ($P < 0.05$).

[c]Significantly different from the maximum response induced by IP-C5 at CHO-hM$_2$-Y104$^{3.33}$A receptors ($P < 0.05$).

n.a., not applicable.

Table 3

Binding characteristics of muscarinic agonists in [^{3}H]NMS displacement studies with living CHO-hM_2 cells

Compound	pK_A Control conditions	Hill slope Control Conditions	Compound	pK_A PTX	Hill slope PTX
Ach (*n* = 3)	5.86 ± 0.04	–0.97 ± 0.07	**ACh (*n* = 4)**	5.66 ± 0.07	–0.92 ± 0.10
Oxo M (*n* = 8)	5.72 ± 0.03	–0.86 ± 0.07	**Oxo M (*n* = 3)**	5.44[b] ± 0.10	–0.93 ± 0.15
IP-C1 (*n* = 3)	7.49 ± 0.16	–0.60[a] ± 0.04	**IP-C1 (*n* = 3)**	7.66 ± 0.08	–0.59[a] ± 0.05
IP-H (*n* = 4)	5.88 ± 0.04	–0.71[a] ± 0.04	**IP-H (*n* = 4)**	5.80 ± 0.03	–0.86[a] ± 0.06
IP-C3 (*n* = 3)	5.38 ± 0.07	–1.00 ± 0.08	**IP-C3 (*n* = 3)**	5.23 ± 0.03	–1.00 ± 0.09
IP-C5 (*n* = 3)	5.09 ± 0.05	–1.06 ± 0.11	**IP-C5 (*n* = 3)**	5.03 ± 0.05	–1.05 ± 0.15
C1-IP-C1 (*n* = 4)	5.14 ± 0.12	–0.89 ± 0.14	**C1-IP-C1 (*n* = 4)**	4.89 ± 0.10	–0.97 ± 0.14

Equilibrium binding dissociation constants (minus log values, pK_A) and slope factors were obtained from fitting the four parameter logistic equation to data from individual experiments (Figure 2C) conducted with CHO cells without (left panel) and with PTX pretreatment (right panel). Data are means ± SEM from *n* (as indicated below the agonist name) independent experiments conducted in triplicate. pK_A of ACh and IP-C1 were taken from Bock *et al.* (2012).
[a]Significantly different from –1 ($P < 0.05$).
[b]Significantly different from control condition ($P < 0.05$).

methacholine at the M_4, but not the M_2 receptor, in a cAMP-accumulation assay.

Substitution of one methyl residue either by hydrogen (yielding IP-H) or by an elongated alkyl residue (IP-C3, IP-C5) considerably reduces potency relative to iperoxo. Thus, the trimethylated quaternary nitrogen appears to play a key role for iperoxo's high potency. However, the quaternary trimethylammonium residue is also contained in ACh and oxotremorine M. Therefore, receptor interaction of this moiety *per se* would not explain the high potency of iperoxo. In fact, the pronounced loss of potency by about three log-units caused by methylation of iperoxo's isoxazoline ring (see C1-IP-C1 in Figures 1 and 2B) demonstrates the importance of the unchanged ring for the iperoxo–receptor interaction.

In order to quantify efficacies of the probes for G_i and G_s pathway activation in the DMR assay, we determined the affinity of test compounds to hM_2 receptors and the number of cell surface receptors (268 000 ± 37 000 receptors per CHO cell without and 222 000 ± 23 000 receptors per cell with PTX pretreatment; not significantly different). To this end, we measured displacement of the quaternary, non-permeant [^{3}H]*N*-methylscopolamine ([^{3}H]NMS) from living CHO-hM_2 cells. The affinity of the radioligand [^{3}H]NMS was slightly enhanced after the pretreatment with PTX, perhaps because NMS is an inverse agonist [pK_D (control) = 9.23 ± 0.06; pK_D (PTX) = 9.45 ± 0.03; $n = 3$]. PTX pretreatment hardly affects test compound binding (see Figure 2C, iperoxo, and Table 3 for binding data of all test compounds). Test compound-induced displacement of [^{3}H]NMS revealed that the high potency of iperoxo (Figure 2B) is paralleled by a high binding affinity relative to conventional agonists such as ACh (Figure 2C). The curves for iperoxo (and IP-H) are rather shallow (for slope factors, see Table 3), which cannot be mechanistically explained at present. The wide difference between the concentrations of iperoxo for a half maximum effect (about 100 pM, Figure 2B) and for half maximum binding (30 000 pM, Figure 2C) suggests a high operational efficacy of iperoxo (see the following paragraph).

Structure of iperoxo encodes more than physiological efficacy

We analysed test compound-induced DMR according to the operational model of pharmacological agonism (Black and Leff, 1983). This model yields the operational efficacy 'tau, τ' between the test compound-bound receptor and downstream signalling. The fitted curves (Supplementary Figure S3) nicely describe the DMR data from Figure 2B. Taking the inflection points of the whole cell binding curves to estimate agonist binding affinities, log τ values for G_i pathway activation were derived which indicate that iperoxo, IP-H and IP-C3 significantly surpass ACh (and oxotremorine M) in operational efficacy (Figure 3A). Accordingly, IP-H and IP-C3 appear to behave as 'superagonists' with respect to G_i signalling, whereas both IP-C5 and the ring-methylated derivative of iperoxo (C1-IP-C1) do not differ in efficacy from ACh.

In order to exclude that the difference in steepness of the whole cell binding curve between iperoxo and ACh introduces a bias into the calculation of τ, binding curves were additionally generated in cell homogenates under conditions of suppressed G-protein–receptor interaction (high concentration of guanyl nucleotides, PTX pretreatment). Curves were flat for both, iperoxo and ACh, while derived τ values remained significantly different under the applied conditions of G-protein uncoupling (Supplementary Figure S4 and Supplementary Table S1). Notably, other investigators also observed flat agonist binding curves under 'minimized receptor–G-protein association' (for instance, Valant *et al.*, 2008 and references therein).

Binding studies were performed at 28°C, where some receptor internalization may take place (e.g. Maloteaux and Hermans, 1994). As the pK_A of iperoxo and ACh, respectively, did not differ after 1 h and 2 h of incubation (Supplementary Figure S5 and Supplementary Table S3), measurements made after 2 h warrant steady-state conditions. Provided that iperoxo causes more pronounced M_2 receptor internalization as compared with ACh, its binding affinity would be overes-

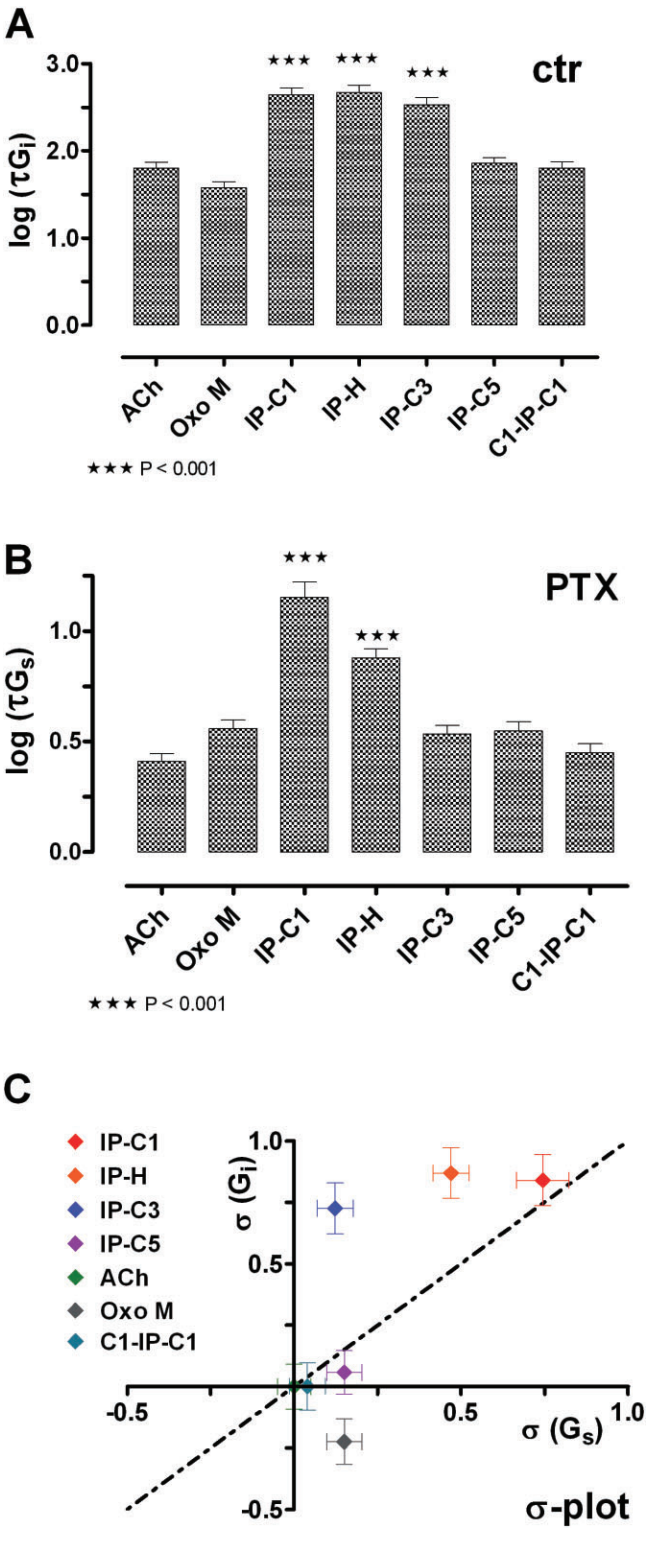

Figure 3

Quantifying test compound signalling in CHO-hM$_2$ cells. Operational efficacies τ for G_i signalling (A) and G_s signalling (B), (***: $P < 0.001$, significantly different from ACh at the M_2 wild-type receptor according to one-way ANOVA with Bonferroni's multiples comparison test). (C) Comparison of effective signalling σ of test compound-bound CHO-hM$_2$ receptors into the G_i- (y-axis) and the G_s pathway (x-axis) respectively. σ expresses test compound operational efficacy relative to the operational efficacy of ACh, the latter defining balanced G_i/G_s signalling, which is indicated by the dashed line. Only in case of IP-C3, the orthogonal distance of the data point from the dashed line is significant, thus indicating G_i bias ($P < 0.05$ according to one-way ANOVA with Bonferroni's multiples comparison test).

timated due to an additional inhibitory effect; thus, operational efficacy of iperoxo would rather be underestimated than overestimated.

Finally, pretreatment of CHO-M_2 with the alkylating agent phenoxybenzamine to irreversibly block part of the receptors reduced the DMR response of ACh relative to iperoxo, suggesting a higher 'receptor reserve' of the latter (Supplementary Figure S6).

With respect to G_s activation (Figure 3B), τ-values are generally lower compared with G_i activation (Figure 3A; note different ordinate scales), reflecting that the former needs higher agonist concentrations than the latter (see Figure 2B).

Worth mentioning the measured maximum of G_s activation by ACh and other compounds (Figure 2B) exceeds the value expected on the basis of the computed τ. According to the limiting value of the effect E, according to the Black and Leff equation,

$$\underset{[A]\to\infty}{E} = \frac{E_{max}\tau}{\tau+1}$$

a $\tau = 2$ (log $\tau_{ACh} = 0.4$, Table 1) should yield E = 2/3 E_{max}. The most likely explanation is that the measured binding constant used for curve fitting does not exactly match the 'microscopic' binding constant of the G_s protein-bound receptor. Nevertheless, such a systematic deviation is not expected to influence the rank order of operational efficacies as computation of τ based on the four measured series of affinity values (Table 3, Supplementary Table S1) consistently ranked iperoxo higher than ACh with regard to G_i activation. In general, our analysis is not based on absolute τ-values, but on rank orders of τ observed under a given experimental condition.

In any case, with respect to G_s activation, iperoxo and IP-H, but not IP-C3, surpass the other test compounds including ACh in efficacy. Furthermore, efficacy for G_s activation of iperoxo is significantly superior to that of IP-C3 ($P < 0.01$, t-test).

We conclude, first, that iperoxo and IP-H are 'superagonists' also with respect to G_s activation. Second, G_s–protein activation by the agonist-bound M_2 receptor is more sensitive to agonist structure than G_i–protein activation. Obviously, small substituents on iperoxo's quaternary nitrogen are a prerequisite for a more than physiological G_s activation, suggesting that a more pronounced contraction of the hydrophobic cage of amino acids that surrounds the positively charged head group (Lu *et al.*, 2002) is required for G_s- compared with G_i–protein activation.

According to Lefkowitz and coworkers (Rajagopal *et al.*, 2011), we use the parameter σ to quantify the signalling pattern of a test compound/receptor complex relative to the ACh-bound M_2 receptor. The latter defines 'balanced' G_i/G_s

signalling as ACh is the physiological receptor activator. In the σ-plot (Figure 3C), balanced signalling is reflected by the angle bisector, which runs through the origin defined by the endogenous activator. The data point of iperoxo nicely meets the diagonal. This indicates that efficacy of iperoxo for the two pathways is proportionally increased relative to ACh. IP-C3 is G_i-biased as it preserves 'G_i superagonism', whereas efficacy for G_s signalling is on the level of ACh. Further elongation of the *N*-alkyl substitutent to IP-C5 yields ACh-like signalling properties. On the other hand, regarding the tail of iperoxo, introduction of a methyl group reduces efficacies for both pathways to the ACh level. Taken together, these data demonstrate that both ends of the iperoxo molecule contribute to its 'superagonism'. Appropriate modification of either end (i.e. the quaternary ammonium head or the isoxazoline ring tail) reduces signalling competence to the level of ACh.

Iperoxo resists an orthosteric loss-of-function mutation

Findings reported above suggest that an interaction of the quaternary head group of iperoxo with the region around M_2-D103$^{3.32}$ is one component of at least two agonist–receptor interactions underlying enhanced efficacy relative to ACh. In order to further substantiate this concept, a mutant next to the essential D103$^{3.32}$ was applied (i.e. M_2-Y104$^{3.33}$A), which has proven useful for probing orthosteric interactions (Antony *et al.*, 2009; Gregory *et al.*, 2010). According to radioligand binding in membranes of transfected CHO cells, iperoxo and ACh lose affinity by three log-units in this mutant relative to M_2 wild-type (Antony *et al.*, 2009). In the present study, DMR reveals that the potency of iperoxo for inducing positive DMR falls remarkably by five log-units in the receptor mutant (Figure 4A,B) relative to M_2 wild-type (Figure 2B). PTX pretreatment to chemically knock-out G_i signalling shows that G_s signalling is hardly visible in the range of applied iperoxo concentrations (Figure 4A). Yet, if the potency of iperoxo for triggering G_s signalling is likewise diminished by five orders of magnitude as found for the G_i response (see above), G_s activation would take place beyond the applied concentration range. Therefore, we cannot decide whether G_s activation is extinguished by the mutant or not. With respect to the G_i response, iperoxo, IP-H, IP-C3 and IP-C5 lose potency in DMR experiments at M_2-Y104$^{3.33}$A relative to wild-type by about five, three, two and one log-units respectively (compare Figure 2B with Figure 4B and Tables 1 with 4). These structure potency loss relationships are in line with the finding (see above) that substitution of a methyl residue by a hydrogen atom or by *n*-propyl and *n*-pentyl increasingly weakens the receptor interaction of the quater-

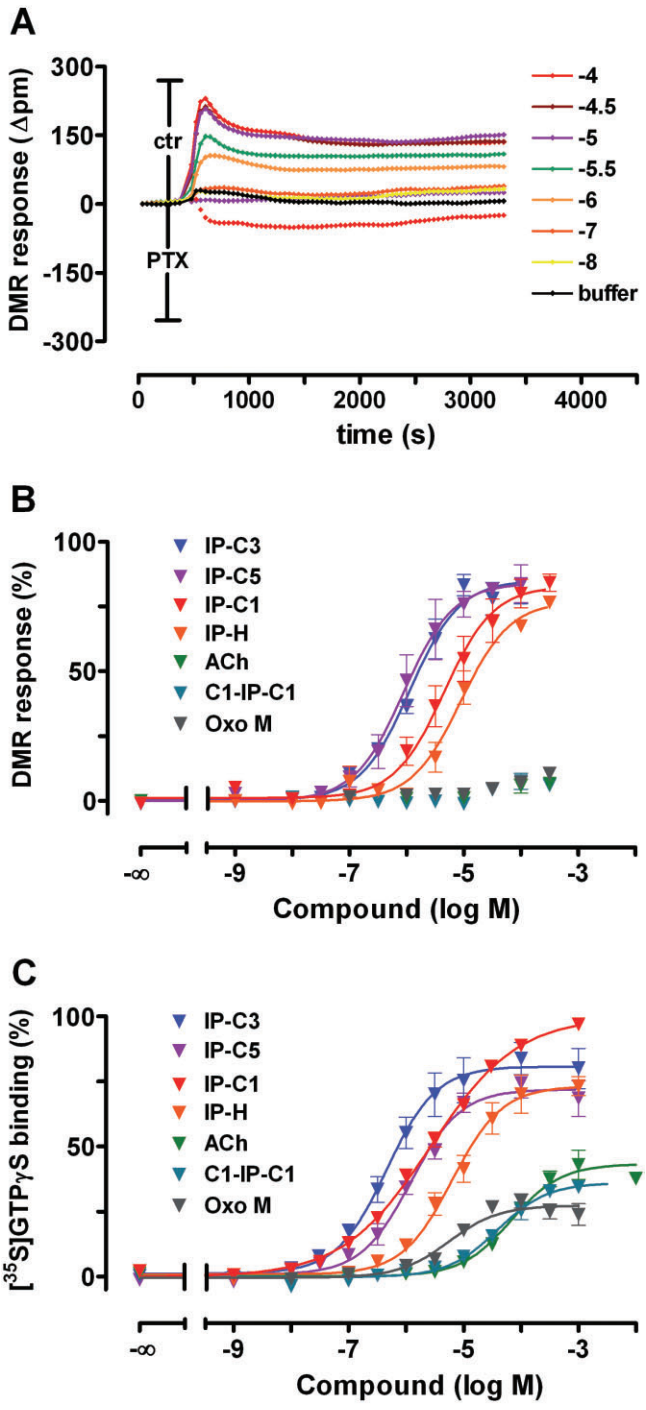

Figure 4

An orthosteric loss-of-function mutation directly demonstrates enhanced efficacy. (A) Original recordings of iperoxo-induced DMR in CHO-hM_2-Y104$^{3.33}$A cells without and with PTX-pre-treatment. Shown are mean values of a quadruplicate determination of a representative experiment that was repeated four times with similar results. SEM did never exceed 20 pm. Note that PTX pretreatment almost abolished G_s signalling. (B) Concentration–DMR curve of test compound-induced G_i signalling in CHO-hM_2-Y104$^{3.33}$A cells. Curve fitting based on the four parameter logistic function. Data from individual experiments were normalized to the maximum response induced by iperoxo in the respective experiment at the CHO-hM_2 wild-type receptor. Shown are means ± SEM of three to five independent experiments conducted in quadruplicates. (C) Agonist-induced [^{35}S]GTPγS binding reflecting G_i signalling in membrane homogenates of CHO-hM_2-Y104$^{3.33}$A cells. Data from individual experiments were normalized to the maximum response induced by iperoxo in the respective experiment at the CHO-hM_2-Y104$^{3.33}$A receptor. Shown are means ± SEM of three to seven independent experiments.

Table 4

DMR in M_2-Y104$^{3.33}$A cells induced by muscarinic agonists

Compound	pEC_{50}	E_{max} (%)	Hill slope
ACh (n = 5)	n.a.	8 ± 5	n.a.
Oxo M (n = 3)	n.a.	13 ± 2	n.a.
IP-C1 (n = 5)	5.24 ± 0.20	83 ± 3	0.74 ± 0.16
IP-H (n = 3)	5.07 ± 0.12	77 ± 3	1.53 ± 0.31
IP-C3 (n = 3)	5.99 ± 0.11	83 ± 2	1.21 ± 0.23
IP-C5 (n = 3)	6.02 ± 0.22	84 ± 3	1.07 ± 0.23
C1-IP-C1 (n = 3)	n.a.	8 ± 2	n.a.

Agonist concentrations inducing the half maximal effect in concentration–DMR curves as measures of agonist potency (minus log values, pEC_{50}), maximum agonist effects (E_{max}) and slope factors were obtained by fitting the four parameter logistic equation to data from individual experiments shown in Figure 4B.

E_{max} values are expressed in % of the maximum response induced by iperoxo at the CHO-hM_2 wild-type receptor on the same 384-well plate.

Data are means ± SEM from n (as indicated below the agonist name) independent experiments conducted in quadruplicate.

Since ACh, Oxo M and C1-IP-C1 dramatically loose efficacy at the mutant receptor, no curve fitting was possible with these three compounds.

nary head group. As a consequence, mutation of the corresponding structural element of the receptor has less effect on potency.

The absolute maximum of DMR (upper plateau in Figure 4B) induced by iperoxo and its derivatives in CHO-hM_2-Y104$^{3.33}$A cells almost equals the effect observed in CHO-hM_2 wild-type cells. ACh, oxotremorine M and the ring-methylated iperoxo-derivative (C1-IP-C1), however, fail to induce a clear DMR signal in the CHO-hM_2-Y104$^{3.33}$A cells (Figure 4B). Direct measurement of G_i-protein activation using [^{35}S]GTPγS binding reveals a weak maximum effect of ACh, oxotremorine M and C1-IP-C1 for G_i activation in the mutant amounting to 30–40% relative to iperoxo (Figure 4C, Table 2). In contrast, the head group-modified iperoxo derivatives preserve a considerably higher E_{max} of about 70–80%. As the maximum effects of all test compounds remain below the maximum effect of iperoxo, there is no receptor reserve left for these compounds in this system. Therefore, the CHO-hM_2-Y104$^{3.33}$A mutant provides an experimental condition that – by mere inspection of the maximum effect – directly discloses the higher efficacy of iperoxo and its derivatives relative to ACh. Among the iperoxo derivatives, the most pronounced loss of efficacy occurs with the ring-methylated analogue of iperoxo, C1-IP-C1. This compound suffers from a loss of efficacy to the same extent as ACh does, whereas iperoxo and its congeners with modified head group preserve rather high efficacy at the M_2-Y104$^{3.33}$A mutant (as mentioned above). We conclude that iperoxo and its head group-modified congeners exploit at least one additional epitope for receptor activation apart from the area around M_2-Y104$^{3.33}$. This additional epitope appears to have high physicochemical complementarity to iperoxo's isoxazoline ring, as ring methylation completely reduces efficacy to the level of ACh.

Iperoxo engenders high efficacy in native cells

In order to check for 'superagonism' in another more physiological cellular context, we applied MRC-5 human lung fibroblasts, which express predominantly M_2 receptors (Matthiesen *et al.*, 2006). Muscarinic agonists including iperoxo induce positive DMR (Figure 5A) that is abolished by PTX pretreatment to zero DMR (Figure 5A) and thus reflects G_i activation. This indicates that G_s pathway activation controlled by M_2 receptors is not operative in these cells. As lung fibroblasts express nonspecific cholinesterase (Kris *et al.*, 1994), ACh cannot be applied as the endogenous reference comparator. As shown above (Figures 2 and 3), efficacies for G_i and G_s activation in DMR experiments are not significantly different between oxotremorine M and ACh. Therefore, oxotremorine M was taken as the reference in this part of the study (Figure 5B–D).

Measurement of cell surface binding (Figure 5C) (21 000 ± 8000 receptors per MRC-5 cell) and data analysis based on the operational model yielded operational efficacies τ for both agonists in MRC-5 human lung fibroblasts. Iperoxo significantly surpasses oxotremorine M in efficacy (Figure 5D, Supplementary Table S2). The ratio of τ-values found in MRC-5 is identical to that found in CHO-hM_2 (Figure 3B). Taken together, elevated efficacy of iperoxo is preserved in native cells that do not overexpress muscarinic receptors.

Discussion

A 'superagonist' has been defined as an agonist capable of activating the receptor with higher efficacy than the endogenous activator (Smith *et al.*, 2011). The present study is the first to show that the muscarinic M_2 ACh receptor allows more efficacious activation than that induced by the endogenous agonist. The highly potent agonist iperoxo and less potent derivatives can be classified as muscarinic 'superagonists' under three conditions (i.e. first in CHO cells overexpressing human M_2 receptors, second in a hM_2 receptor point mutant with severely compromised function of the orthosteric site and third in native cells).

Until now, GPCR 'superagonism' has rarely been reported (e.g. Engström *et al.*, 2005; Mistry *et al.*, 2005; and for review Smith *et al.*, 2011) and even less been demonstrated. We suggest that this has methodological reasons. It is an often made observation that activation of a fraction of receptors is sufficient for a full cellular response. This phenomenon is addressed as 'receptor reserve', 'spare receptors' or 'signal amplification' (e.g. Hill *et al.*, 2010; Rajagopal *et al.*, 2011). The phenomenon indicates that it is the signal transduction mechanism that limits the maximum response rather than the number of available receptors. Under such conditions, the maximum response will not differ between a 'superagonist' and the physiological agonist. As conventional pharmacological characterization of a receptor activator in drug discovery is carried out in terms of potency (concentration for a half maximum effect) and the maximum effect, 'superagonism' is prone to being overlooked. Receptor binding

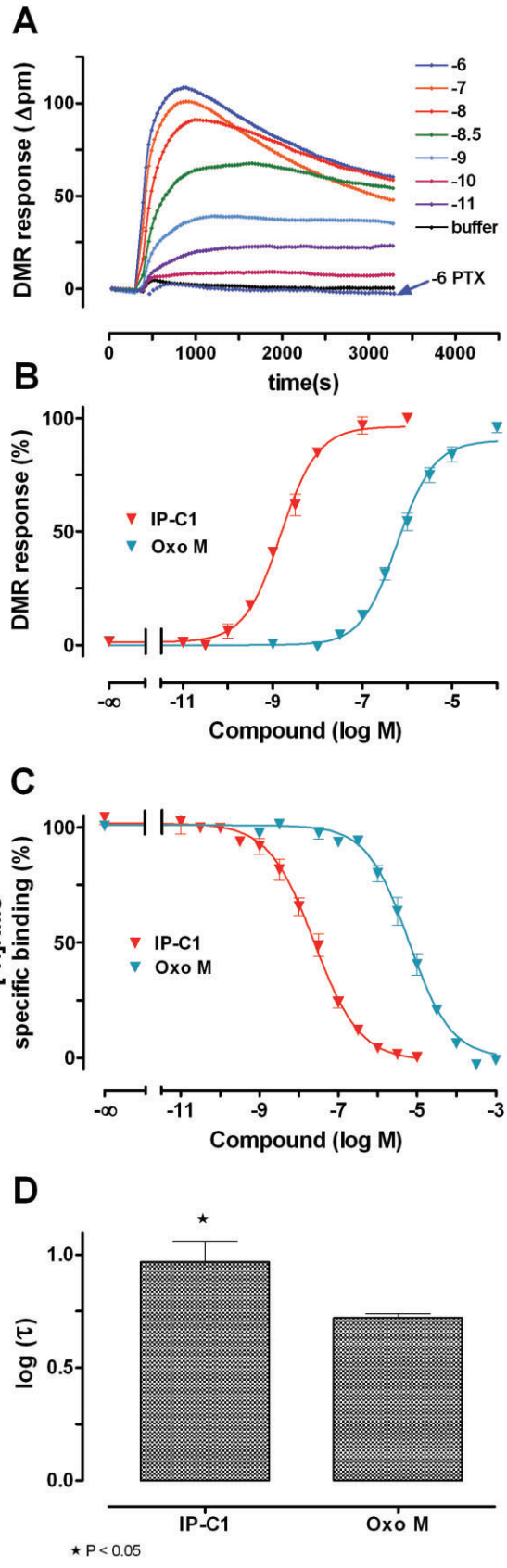

Figure 5

Enhanced efficacy in primary cells (MRC-5). (A) DMR induced by iperoxo in M_2-expressing MRC-5 cells without and with PTX pretreatment. Shown are mean values of a representative experiment carried out in quadruplicate, which was repeated four times with similar results. SEM did never exceed 20 pm. (B) Concentration–DMR curves of iperoxo and oxotremorine M. Curve analysis is based on the four parameter logistic function. Shown are means ± SEM of four to six independent experiments conducted in quadruplicates. (C) Cell surface binding of iperoxo and oxotremorine M as revealed by the displacement of [^{3}H]*N*-methylscopolamine from living MRC-5 cells under conditions of DMR measurements. (D) Operational efficacies τ of agonist-bound M_2 receptors in MRC-5 cells derived from curve fitting to DMR data (cf. panel B) are indicated according to the operational model of Black and Leff (1983), including live cell binding constants (cf. panel C). Operational efficacy τ of iperoxo was significantly higher compared with oxotremorine M (P = 0.011, two-tailed Student's *t*-test).

measurement is crucial to disclose that less receptor occupancy is needed compared with the physiological agonist for inducing the same cellular response. This reflects that the 'superagonist'-bound receptor has a higher operational efficacy τ than the physiological agonist-bound receptor. Worth mentioning, 'superagonism' of iperoxo was not revealed in a previous study, focused on signalling bias, when not only τ but also K_A were variables (Bock *et al.*, 2012).

We suggest implementation of operational efficacy as a parameter in drug discovery. It will be interesting to see if a more frequent quantification of drug action in terms of τ will go along with a more frequent identification of 'superagonism'.

With respect to structure–function relationships, our findings indicate that iperoxo and related compounds utilize an additional 'accessory' interaction point on the receptor protein that is involved in binding to and activation of the receptor protein. All tested compounds share a positively charged 'head' that is important for the interaction with the receptor area around M_2-D103$^{3.32}$ (Lu *et al.*, 2002). Tetramethyl-ammonium is sufficient for muscarinic receptor activation (e.g. Day and Vane, 1963; Hobbiger *et al.*, 1969; Kennedy *et al.*, 1995; Valant *et al.*, 2008). The CHO-hM_2-Y104$^{3.33}$A mutant serves to severely weaken but does not fully eliminate the interaction with this 'classical activation site' (Antony *et al.*, 2009; Gregory *et al.*, 2010). On this mutant, both, ACh and the ring-methylated iperoxo derivative C1-IP-C1 lose about 3 log-units of potency (Table 2). In addition, the efficacy of both of these agonists for receptor activation is strongly attenuated (Figure 4B,C). In contrast, the maximum effect of iperoxo and its *N*-alkylated derivatives is little affected by weakening the 'classical activation site'. One could argue, that iperoxo's 'superagonism' may relate to a different binding topography with less dependency on M_2-Y104$^{3.33}$ in comparison with ACh. However, iperoxo's potency is compromised even more than the potency of ACh, proving that both compounds strongly depend on the M_2-Y104$^{3.33}$. Potencies of iperoxo and its congeners respond differently to the mutation, depending on the substitution pattern of the compounds' positively charged head (compare Figures 2B with 4B), but eventually fall to the same level of low potency at the mutant receptor. Notably, the pronounced loss

of binding affinity resulting from the mutation precludes radioligand binding experiments; therefore, test compounds could not be characterized in terms of affinity and operational efficacy τ, but merely of potency and maximum effect. Importantly, however, evaluation of τ is not required to clearly see 'superagonism' in the particular experimental approach. The 'accessory activation site' involved in iperoxo-mediated activation of the orthosteric mutant has to reside in iperoxo's Δ^2-isoxazolinyl-ether substituent, as this moiety constitutes the only difference in structure to the conventional agonist oxotremorine M (Figure 1). This conclusion is corroborated by introduction of one methyl residue into the isoxazoline ring leading to ACh-like signalling properties (Figures 3 and 4). Receptor activation *via* the 'accessory activation site' explains why iperoxo and its *N*-alkylated derivatives maintain receptor activation, when the 'classical activation site' is incapacitated by mutation. With respect to potency, contribution of the 'accessory activation site' explains why iperoxo and its *N*-alkylated structural analogues preserve a considerably higher potency compared with ACh at the 'classical activation site' mutant (Figure 4C). In line with this, potency of the ring-methylated derivative, C1-IP-C1, falls to the level of ACh, thus highlighting importance of the undisturbed interaction of the isoxazoline ring with the 'accessory site'.

According to this concept, iperoxo is unique compared with conventional agonists such as ACh because of the ability to simultaneously activate at least two adjacent epitopes on the receptor protein. This proposed 'twin activation' mechanism would stabilize conformational oscillations of the agonist-bound receptor at conformations of maximum efficacy for G-protein activation. The complete loss of 'superagonism' observed with the *N*-*n*-pentyl-substituted iperoxo derivative as well as with the ring-methylated iperoxo analogue (Figure 3D) might result from a loss of 'twin activation' capacity, induced by an impaired interaction with either the 'classical activation site' or the 'accessory site'.

'Twin activation' through the 'classical site' is likewise impaired in the CHO-hM_2-Y104$^{3.33}$A mutant. In that case, all compounds carrying the Δ^2-isoxazolinyl-ether moiety are still able to activate the mutant receptor irrespective of the size of the *N*-substituent (Figure 4B). This implies that activation of the 'accessory site' is independent of the 'classical activation site'.

The susceptibility for 'superagonism' discloses that evolution did not optimize the ACh/receptor complex for maximum signalling. One may ask why 'mother nature' operates with an agonist/receptor system that has less than maximal efficacy. Is this a tribute to the ester function of ACh, which allows rapid degradation? Is the conformationally flaccid ACh/receptor complex more sensitive to regulation, for instance by inner loop phosphorylation? Future study is required to find out whether the 'less than possible receptor activation' goes along with a functional advantage. In any case, agonists with a 'better-than-ACh action' may be highly useful as tools for biological research and drug discovery.

Acknowledgement

We thank Corning® Inc. for their support on the Epic® system. This work was funded by the Deutsche Forschungsgemeinschaft (DFG) by grants to KM (MO 821/2-1), UH (HO 1368/12-1), EK (KO 1583/3-1). RS and WKS are members of the graduate school BIGS DrugS, University of Bonn, and Biotech-Pharma, University of Bonn respectively. RS is funded by the German National Academic Foundation.

Conflict of interest

None.

References

Alexander SPH, Mathie A, Peters JA (2011). Guide to Receptors and Channels (GRAC), 5th edition. Br J Pharmacol 164 (Suppl. 1): 1–324.

Antony J, Kellersohn K, Mohr-Andrae M, Kebig K, Prilla S, Muth M *et al.* (2009). Dualsteric GPCR targeting: a novel route to binding and signaling pathway selectivity. FASEB J 23: 442–450.

Black JW, Leff P (1983). Operational models of pharmacological agonism. Proc R Soc Lond B 220: 141–162.

Bock A, Merten N, Schrage R, Dallanoce C, Bätz J, Klöckner J *et al.* (2012). The allosteric vestibule of a seven transmembrane helical receptor controls G-protein coupling. Nat Commun 3: 1044. doi: 10.1038/ncomms2028.

Dallanoce C, Conti P, De Amici M, De Micheli C, Barocelli E, Chiavarini M *et al.* (1999). Synthesis and functional characterization of novel derivatives related to oxotremorine and oxotremorine-M. Bioorg Med Chem 7: 1539–1547.

Day M, Vane JR (1963). An analysis of the direct and indirect actions of drugs on the isolated guinea-pig ileum. Br J Pharmacol Chemother 20: 150–170.

DeBlasi A, O'Reilly K, Motulsky HJ (1989). Calculating receptor number from binding experiments using same compound as radioligand and competitor. Trends Pharmacol Sci 10: 227–229.

Deupi X, Kobilka BK (2010). Energy landscapes as a tool to integrate GPCR structure, dynamics, and function. Physiology (Bethesda) 25: 293–303.

DeWire SM, Ahn S, Lefkowitz RJ, Shenoy SK (2007). β-Arrestins and cell signaling. Annu Rev Physiol 69: 483–510.

Disingrini T, Muth M, Dallanoce C, Barocelli E, Bertoni S, Kellershohn K *et al.* (2006). Design, synthesis, and action of oxotremorine-related hybrid-type allosteric modulators of muscarinic acetylcholine receptors. J Med Chem 49: 366–372.

Engström M, Tomperi J, El-Darwish K, Ahman M, Savola JM, Wurster S (2005). Superagonism at the human somatostatin receptor subtype 4. J Pharmacol Exp Ther 312: 332–338.

Gregory KJ, Hall NE, Tobin AB, Sexton PM, Christopoulos A (2010). Identification of orthosteric and allosteric site mutations in M2 muscarinic acetylcholine receptors that contribute to ligand-selective signaling bias. J Biol Chem 285: 7459–7474.

Haga K, Haga T, Ichiyama A, Katada T, Kurose H, Ui M (1985). Functional reconstitution of purified muscarinic receptors and inhibitory guanine nucleotide regulatory protein. Nature 316: 731–733.

Hill SJ, Williams C, May LT (2010). Insight into GPCR pharmacology from the measurement of changes in intracellular cyclic AMP; advantages and pitfalls of differing methodologies. Br J Pharmacol 161: 1266–1275.

Hobbiger F, Mitchelson F, Rand MJ (1969). The actions of some cholinomimetic drugs on the isolated taenia of the guinea-pig caecum. Br J Pharmacol 36: 53–69.

Jäger D, Schmalenbach C, Prilla S, Schrobang J, Kebig A, Sennwitz M *et al*. (2007). Allosteric small molecules unveil a role of an extracellular E2/transmembrane helix 7 junction for G protein-coupled receptor activation. J Biol Chem 282: 34968–34976.

Kenakin T, Miller LJ (2010). Seven transmembrane receptors as shapeshifting proteins: the impact of allosteric modulation and functional selectivity on new drug discovery. Pharmacol Rev 62: 265–304.

Kennedy RH, Wyeth RP, Gerner P, Liu S, Fontenot HJ, Seifen E (1995). Tetramethylammonium is a muscarinic agonist in rat heart. Am J Physiol 268 (6 Pt 1): C1414–C1417.

Klöckner J, Schmitz J, Holzgrabe U (2010). Convergent, short synthesis of the muscarinic superagonist iperoxo. Tetrahedron Lett 51: 3470–3472.

Kris M, Jbilo O, Bartels CF, Masson P, Rhode S, Lockridge O (1994). Endogenous butyrylcholinesterase in SV40 transformed cell lines: COS-l, COS-7, MRC°5 SV40, and WI-38 VA13. In Vitro Cell Dev Biol 30A: 680–689.

Lagerström MC, Schiöth HB (2008). Structural diversity of G protein-coupled receptors and significance for drug discovery. Nat Rev Drug Discov 7: 339–357.

Lamyel F, Warnken-Uhlich M, Seemann WK, Mohr K, Kostenis E, Ahmedat AS *et al*. (2011). The β2-subtype of adrenoceptors mediates inhibition of pro-fibrotic events in human lung fibroblasts *Naunyn Schmiedebergs Arch*. Pharmacol 384: 133–145.

Lu ZL, Saldanha JW, Hulme EC (2002). Seven-transmembrane receptors: crystals clarify. Trends Pharmacol Sci 23: 140–146.

Maloteaux JM, Hermans E (1994). Agonist induced muscarinic cholinergic receptor internalization, recycling and degradation in cultured neuronal cells. Biochem Pharmacol 47: 77–88.

Matthiesen S, Bahulayan A, Kempkens S, Haag S, Fuhrmann M, Stichnote C *et al*. (2006). Muscarinic receptors mediate stimulation of human lung fibroblast proliferation. Am J Respir Cell Mol Biol 35: 621–627.

Michal P, Lysíková M, Tuček S (2001). Dual effects of muscarinic M_2 acetylcholine receptors on the synthesis of cyclic AMP in CHO cells: dependence on time, receptor density and receptor agonists. Br J Pharmacol 132: 1217–1228.

Milligan G (2003). Principles: extending the utility of [35S]GTPγS binding assays. Trends Pharmacol Sci 24: 87–90.

Mistry R, Dowling MR, Challiss RAJ (2005). An investigation of whether agonist-selective receptor conformations occur with respect to M2 and M4 muscarinic acetylcholine receptor signalling via Gi/o and Gs proteins. Br J Pharmacol 144: 566–575.

Mohr K, Tränkle C, Kostenis E, Barocelli E, De Amici M, Holzgrabe U (2010). Rational design of dualsteric GPCR ligands: quests and promise. Br J Pharmacol 159: 997–1008.

Rajagopal S, Ahn S, Rominger DH, Gowen-MacDonald W, Lam CM, DeWire SM *et al*. (2011). Quantifying ligand bias at seven-transmembrane receptors. Mol Pharmacol 80: 367–377.

Schröder R, Janssen N, Schmidt J, Kebig A, Merten N, Hennen S *et al*. (2010). Deconvolution of complex G protein-coupled receptor signaling in live cells using dynamic mass redistribution measurements. Nat Biotechnol 28: 943–949.

Schröder R, Schmidt J, Blättermann S, Peters L, Janssen N, Grundmann M *et al*. (2011). Applying label-free dynamic mass redistribution technology to frame signaling of G protein-coupled receptors noninvasively in living cells. Nat Protocols 6: 1748–1760.

Smith NJ, Bennett KA, Milligan G (2011). When simple agonism is not enough: emerging modalities of GPCR ligands. Mol Cell Endocrinol 331: 241–247.

Suratman S, Leach K, Sexton PM, Felder CC, Loiacono LE, Christopoulos A (2011). Impact of species variability and 'probe-dependence' on the detection and in vivo validation of allosteric modulation at the M4 muscarinic acetylcholine receptor. Br J Pharmacol 162: 1659–1670.

Tränkle C, Kostenis E, Burgmer U, Mohr K (1996). Search for lead structures to develop new allosteric modulators of muscarinic receptors. J Pharmacol Exp Ther 279: 926–933.

Valant C, Gregory KJ, Hall NE, Scammells PJ, Lew MJ, Sexton PM *et al*. (2008). A novel mechanism of G protein-coupled receptor functional selectivity. Muscarinic partial agonist McN-A-343 as a bitopic orthosteric/allosteric ligand. J Biol Chem 283: 29312–29321.

Valant C, Lane RJ, Sexton PM, Christopoulos A (2012). The best of both worlds? Bitopic orthosteric/allosteric ligands of G protein–coupled receptors. Annu Rev Pharmacol Toxicol 52: 153–178.

Supporting information

Additional Supporting Information may be found in the online version of this article at the publisher's web-site:

Figure S1 (A) HCHO (40% aq.), $HN(CH_3)_2$ × HCl, $CuSO_4$ × $5H_2O$; (B) $NaNO_2$/DMSO; (C) NaH, abs. THF; (D) R–X, $CHCl_3$, r.t. or 55°C; (E) CH_3I, Et_2O/acetone (1:1), r.t.

Figure S2 DMR induced by the indicated concentrations of ACh. Original recordings of ACh-induced DMR (expressed as Δpm wavelength shift) from a representative experiment. Similar to the DMR induced by iperoxo (cf. Figure 2A), ACh induces positive DMR in CHO-hM_2 cells, including a characteristic G_i-peak under normal conditions (upper panel, solid lines) or negative DMR after pretreatment with PTX to inactivate G_i and thereby uncover G_s-protein signalling (lower panel, dashed lines). Shown are mean values of quadruplicate determinations from one out of four experiments with similar results. SEM was always below 25 pm.

Figure S3 Test compound-induced DMR in CHO-hM_2 cells reflecting G_i- ('ctr') and G_s- ('PTX') activation (data from Figure 2B) was analysed according to the operational model of agonism (Black and Leff, 1983), including live cell binding constants (Table 3).

Figure S4 Influence of guanylnucleotides and PTX on binding of iperoxo (left) and to ACh (right) to muscarinic M_2 receptors in cell homogenates reflected as displacement of the radiolabelled orthosteric antagonist *N*-methylscopolamine ([^{3}H]NMS).

Figure S5 Whole cell binding assay terminated at two different time points to verify steady-state conditions. Cell surface binding of iperoxo (IP-C1) and ACh as reflected by displacement of [^{3}H]NMS after 1 h and 2 h (taken from Figure

2C). Curve fitting based on the four parameter logistic function. Shown are means ± SEM of three to four independent experiments conducted in triplicate.

Figure S6 Influence of receptor alkylation on test compound-induced DMR. Maximum DMR induced by iperoxo (IP-C1), pilocarpine (Pilo) and ACh without and with pretreatment with the alkylating agent phenoxybenzamine (Pbz) 1 μM for 30 min (according to Antony *et al.*, 2009 and references therein). The applied test compound concentrations of IP-C1 and ACh exceeded the respective inflection points of the concentration–effect curves ('ctr' in Figure 2B) by a factor of 1000. After pretreatment with Pbz, cells were washed trice with assay buffer and DMR was measured (cf. Methods). The test compound-induced maximum DMR in the first 1800 s is expressed in percent of the maximum DMR induced by 100 nM IP-C1 in the respective assay. The partial agonist pilocarpine was used to verify successful receptor blockade. In two out of four independently conducted experiments, this prerequisite was fulfilled. Shown are means ± SEM of these two (A and B) independent experiments conducted at least in quadruplicate. $^{n.s.}$ not significantly different from the respective effect of IP-C1 100 nM. *,**,*** significantly different from the respective effect of IP-C1 100 nM (*$P < 0.05$, **$P < 0.01$, ***$P < 0.001$).

Table S1 Agonist binding constants under three different conditions for inhibition of G-protein coupling with the muscarinic M_2 receptor (cf. Supplementary Figure S4) and corresponding operational efficacies τ in DMR (cf. Supplementary Figure S3). Equilibrium binding constants (minus log values, pK_A) and slopes of the agonist binding curve (Hill slope) were derived from fitting the four parameter logistic function to data.

Table S2 Overview over binding and functional data of iperoxo in comparison to oxotremorine M obtained at human lung fibroblasts (MRC-5).

Table S3 Parameter values of agonist binding after 1 h of incubation (cf. binding curves in Supplementary Figure S5).